CrossMark

2D and 3D Terahertz Imaging and X-Rays CT for Sigillography Study

M. Fabre [1] · R. Durand [2] · L. Bassel [3] · B. Recur [4] · H. Balacey [2] · J. Bou Sleiman [2] · J.-B. Perraud [2] · P. Mounaix [2]

Abstract Seals are part of our cultural heritage but the study of these objects is limited because of their fragility. Terahertz and X-Ray imaging are used to analyze a collection of wax seals from the fourteenth to eighteenth centuries. In this work, both techniques are compared in order to discuss their advantages and limits and their complementarity for conservation state study of the samples. Thanks to 3D analysis and reconstructions, defects and fractures are detected with an estimation of their depth position. The path from the parchment tongue inside the seals is also detected.

Keywords Tomography · Terahertz imaging · 3D reconstruction · Time of flight · THz computed tomography · Nondestructive testing · Spectro imaging · Reflection and transmission images · Sigillography · Ancient seals · Seals-Archeometry

1 Introduction

The significance of enhancing the knowledge of materials and hidden layered materials is important for the preventive conservation of our cultural heritage and the technical history. In the field of terahertz science, the main difficulties lie in the deployment of acquisition routines compatible with the severe constraints induced by the status of public archives (i.e., the

✉ P. Mounaix
patrick.mounaix@u-bordeaux.fr

[1] Centre de Recherche Bretonne et Celtique (EA 4451) Université de Bretagne Occidentale, 20 rue Duquesne, 29238 Brest Cedex 3, France

[2] IMS, Université de Bordeaux/UMR CNRS 5218, 351 Cours de la Libération, 33405 Talence Cedex, France

[3] IRAMAT-CRP2A, UMR CNRS 5060, Université Bordeaux Montaigne, Maison de l'Archéologie, Domaine Universitaire, Esplanade des Antilles, 33607 Pessac Cedex, France

samples under investigation). For example, it is imperative to perform experiments on site and to assume the specimen under scrutiny safety (non-damaging analysis). In any case, diagnosis of patrimonial documents and objects [1] is challenging since i) the examining of these fragile historical artifact has to be done with caution, and ii) the test is required to be completed on site and not in a laboratory environment. To illustrate this purpose, Jackson et al. performed Terahertz (THz) examination of wall painting and drawing [2]. Utilizing THz time domain spectroscopy (THz-TDS), they uncovered the nearness of a graphite drawing [3] under layers of paint and mortar. Concerning art painting, Adam and colleagues looked at THz reflection pictures of shrouded paint layers [4]. Also, a comparative study was exhibited by Fukunaga and collaborators to measure the transmittance of few pigments [5]. Recently, they prolonged their work to a medieval manuscript [1] and even mummies have been studied by THz imaging [6]. All these applicative studies clearly demonstrate the potential of THz imaging for historical, archeological sciences and art [7–9].

THz spectroscopy associated with THz imaging holds large potential in the field of nondestructive, contact-free testing. The constant advances in the development of THz systems, as well as the appearance of the first related commercial products, indicate that large-scale market introduction of THz systems is rapidly approaching. Nowadays, there is a considerable interest in tomographic methods for THz imaging [10–12] by adding the third dimension for analyzing different samples. Short pulses of broadband THz, continuous wave sources, and microwaves [8] are used to illuminate the target [13]. Coherent detection methods allow the reflected or transmitted THz pulse profile to be measured, and then it is possible to access to the dielectric properties without using Kramers-Kronig relationship [14].

In the art science, the analysis of seals, known as sigillography within historical sciences, focuses on the science that studies the manifold aspects of the seals such as the knowledge of the artifacts (seal impression and seal die). Sigillography represents an attractive historical and archeological research field [15]. Seals are signs of power born in the cultural community of the Near-East, where they are documented from the seventh millennium BC. Then, they gradually released in the Far-East and the West. A seal represents a person of authority, physical person or institution, and serves as a probationary instrument or as a quality label. In the Western countries, an impression is commonly obtained by pressing a seal die, engraved with a negative image, on a malleable material such as clay, wax, lead, gold, silver, or bread, for instance.

Moreover, seals are affixed to any kind of evidence under control in the European legal system. Attached to records, seals are a documentary dated source (place and time). They identify their owner by a codified image whose use is international. As a symbolic gesture, frequently, a fingermark is signed to the back of the wax impression and, sometimes, a lock of hair may have been put into the wax. Dermatoglyphic prints resulting of the most precise fingermarks and locks constitute human biological material and anthropometric dated data. But, also, waxes conserve animal and vegetable materials (hairs, silk, linen, hemp, wool, leather, wood, leaves, pollens, pigments, etc.), used in the manufacturing of the seal or inherent to materials or, rarely, as impurities. As a consequence, seal analysis may help to understand the social life and the organization of an ancient cultural community and may provide technical environment and anthropological data. In short, seals are a promising research field aiming at discovering a lot of information concerning the human, social, and research fields.

By nature, seal impressions are fragile. Then, their fragility must be duly taken into account when they are investigated to preserve this source of history. In order to analyze or image these delicate samples, one can possibly use infrared, visible light, and/or X-Rays. Recently,

terahertz time-domain spectroscopy and imaging (THz-TDI) have become an interesting and powerful tool for nondestructive testing since they allow to both visualize the inner parts of the samples and to map sample chemical composition. Indeed, THz waves display attractive features such as good penetration depth, low scattering, free-space propagation, low photon energy, good beam coherence and broad spectral bandwidth. Since many materials exhibit spectral fingerprints in the THz range, spectroscopic analysis in this region has received much interest as a new efficient and complementary tool for material characterization [7, 16]. Furthermore, the availability of coherent measurements has made THz imaging an attractive noncontact, nonionizing method for a variety of applications.

As an illustration, we demonstrated in a previous work [17] that the absorption of some types of waxes was low enough to perform THz imaging as well as X-Ray computed tomography (CT). In conventional radiology, the X-Ray beam projected on the planar detector accumulated shadows of the components of the object it passes through. In this case, low density elements are totally masked by the shadow of denser elements. 3D X-Ray CT scanner overcomes this drawback since it allows a 3D inspection by extracting successive slices through the object. Indeed, after recording radiographs at different viewing angles, CT reconstruction builds a 3D digital representation of the acquired object which can be sliced in stack of 2D images in any direction by a data processing technique. In addition, 3D image visualization tools may help at investigating the totality of the digital object as well as offering the ability to change, on demand, transparency of its components. However, in the case of low density materials, X-Ray contrast is often not high enough to discriminate two different materials. Thus, we concentrate on studying some relevant samples to establish that THz spectro-imaging and tomography are a good alternative to X-Ray for nondestructive testing of soft materials.

Consequently, in this paper, we present the results after imaging four relevant seals with a THz reflection or transmission imaging module and an X-Ray scanner. We demonstrate that the combination of these methods gives access to both better understanding and conservation state evaluation of these fragile materials. Among all the needed inspection controls, defect detection, as well as dimensional measurements of inner complex geometry, has to be considered. Then, we illustrate that THz imaging can be used to analyze geometrically such complex objects. Moreover, THz tomographic techniques have recently been used to recover three-dimensional images, to perform volumetric spectral analysis [18–20] or to localize defects using the THz frequency range [21]. Thus, 3D tomographic reconstructions of seals are also performed from both X-Rays and terahertz radiographs and processed by an auto-mated segmentation tool [14]. A special attention is brought on fractures and foreign matters.

2 Materials and Methods

2.1 Experimental Setup

THz imaging measurements were made either in reflection mode in the horizontal plane or in transmission mode in the vertical plane. The transmission mode setup is available when including in the spectroscopy main module a specific sample holder. The 2D reflection imaging system is a module part of a TPS 3000 or TPS 4000 (TeraView Ltd, UK) spectrometer with a typical useful bandwidth from 0.1 up to 3 THz. The enclosed optical system contains a Ti: Sapphire mode-locked laser which emits near infrared radiation (800 nm) with sub-100
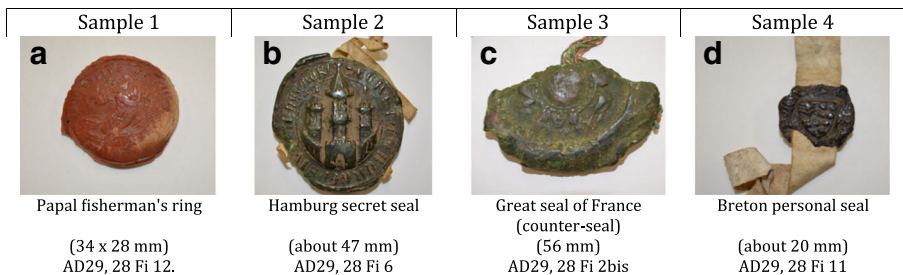
femtosecond pulse duration at a repetition rate of 80 MHz. The average output power is about 300 mW. The laser output is split into pump and probe beams. The pump is focused onto a photo-switch for the generation of the THz field. The reflection geometry is such that the THz beam is focused onto a sapphire window (on which the sample sits) with an angle of incidence of 8°. We carried out several measurements on samples flat enough, and data extraction are proceeded following [22]. In transmission mode, the THz field is transmitted through the sample and is detected with a photo-switch triggered by the probe laser beam. Upon its interaction with the sample, the time-resolved field variation is measured using the probe laser beam into the detector made of a LT-GaAs semiconductor. Finally, the photocurrent induced by the probe laser beam is filtered out and amplified. The time delay line allows sampling the signal step by step and then rebuilding the THz field by a photoconductive sampling technique (optical sampling, based on the use of photoconductive switches: the short laser pulse opens an electrical circuit for a very short time during which the current intensity is measured according with the current optical delay line position). In order to minimize noise effects, all the signals processed in this study correspond to the average of 50 acquisitions. The measurements are carried under dry air. A hygrometer controls in real-time the relative humidity level, which is kept below 1% by using a flow of dry air.

Standard X-Ray datasets exploited in the following have been performed by a Siemens Somaton Sensation open medical X-Ray scanner, provided by TomoAdour company. Moreover, micro-CT scans have been performed at the PACEA UMR 5199 facility, deployed for high-resolution 2D and 3D inspection (at few micron resolution), and metrology. Scan duration varies substantially between each scanning instrument and also depends on the desired resolution and acquisition field-of-view. 3D tomographic reconstructions have been performed by a tomographic software associated to each device.

2.2 Samples

The samples we worked with are included in an untied seal collection preserved in the *Archives départementales du Finistère* (AD29, 28 Fi) [23]. We focused particularly on four of them because of their different aspects and morphology (cf. Fig. 1).

The first one is a seal of Pope Innocent XIII (1721–1724), datable by his pontificate, species of the fisherman ring. It is a red vegetable wax seal, showing St. Peter fishing with a net and a legend around, INNOCENTIUS • P(a)P(a) • XIII, without track of the attaching (oval module, size: 34 × 28 mm), AD29, 28 Fi 1.

Sample 1	Sample 2	Sample 3	Sample 4
a	**b**	**c**	**d**
Papal fisherman's ring	Hamburg secret seal	Great seal of France (counter-seal)	Breton personal seal
(34 x 28 mm) AD29, 28 Fi 12.	(about 47 mm) AD29, 28 Fi 6	(56 mm) AD29, 28 Fi 2bis	(about 20 mm) AD29, 28 Fi 11

Fig. 1 **a** *Papal seal*, *red wax* (1721–1724). **b** Hamburg seal, *green wax* (fourteenth/fifteenth century). **c** Counter-seal on the back of the Great seal of France, *green wax* (Ancient Regime). **d** Breton Guyomar de Lesguen seal, *brown wax* (early fifteenth century), their brief analysis and legal references

The second is a seal of the city of Hamburg (fourteenth/fifteenth century). It is a green composite beeswax pendent seal on doubled tag (round module, size: about 47 mm). AD29, 28 Fi 12. It is the secret seal of the burghers of Hamburg, an architectural seal. A legend, SECRETUM BURGENSIV[…]E HAMBORG, can be read on the external circle, and a town wall with three towers is printed. A fingermark is present on the back.

The third is a royal seal of France (Ancient Regime), species of the Great seal, with a counter-seal. It is a green composite beeswax pendent seal on green and red silk cord (round modules, sizes: >70 mm and about 56 mm). It represents a seal of majesty, showing a seated king, with on the back a heraldic counter-seal. AD29, 28 Fi 2 and 2bis. This seal is very thick, and we can only analyze it on a small thickness. The roughness is also very important.

The fourth is the seal of Guyhomar de Lesguen, a Breton (early fifteenth century); it is a private individual seal, a heraldic seal. It is a brown composite beeswax pendent seal on a tongue (round module, size: about 20 mm). AD29, 28 Fi 11.

Three of these seals contain some foreign matters. Both the Hamburg and Guyhomar seals contain parchment crossing them, and the Great seal contains silk fibers. Each sample was imaged with THz and X-Ray devices described in a previous section.

3 Results

In the following, we detail the specific properties that are revealed from X-Ray and THz acquisitions and the resulting analysis that has been performed depending on the thickness, the shape, and the material of each seal.

3.1 Papal Seal (Sample 1)

It is very fine (few mm) but also very bulging. This important curvature is presented in Fig. 2 which is a comparison between X-Ray images and a B Scan obtained by a 2D terahertz image in reflection mode. Let us recall that THz pulsed imaging can provide a 3D image "map" of the object by using the time-of-flight of the reflected or transmitted THz pulses [24]. In brief, a THz pulse is focused onto the sample and the reflected beam is measured in amplitude and phase. The temporal position of the reflected pulses directly highlights the interfaces, defects, or anomalies from dielectric point of view, along the propagation direction of the beam. In this way, by using the difference of time-of-flight from pixel to pixel, depth information of the 3D profiles of the target can be deduced by a B-Scan technique as in ultrasound microscopy (B-Scan is a 2D cross section in the X-Time or Y-Time planes, and time is equivalent to Z). In
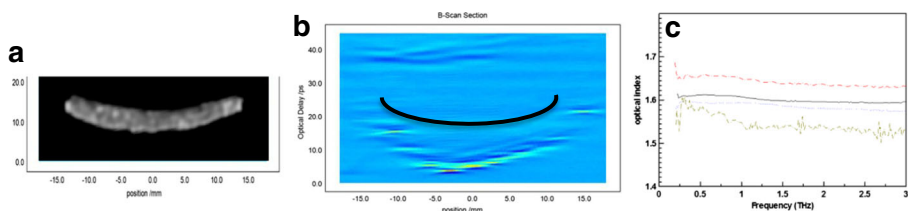
Fig. 2 Comparison between **a** X-Ray image and **b** THz B-Scan of sample. **c** Optical index on several positions in reflection spectroscopy

Fig. 2, we reported the temporal position of the maximum and we correlated this information in depth unity. A quite similar shape is found with time of flight technique.

With this curvature shape determination, a direct consequence is that refractive losses take place and some artifacts in two 2D imaging are quite important for a quantitative determination of the dimensions. By the combination of terahertz spectroscopy and time of flight characteristics, we evaluate the thickness of the seal varying between 2.3 and 2.8 mm. The optical index in THz range is about 1.6 as depicted on Fig. 2c where extraction of optical properties at several positions are reported. That is in a good agreement with measurements carried out with a caliper when possible.

To analyze THz data and propose the best images, we integrate advanced visualization and classification methods [25] which allow us extracting efficiently the information of interest in a big quantity of collected data. We automate various visualization techniques based on time-domain data and frequency domain. Moreover, we add some statistical tools such as principal components analysis (PCA) and Shannon Entropy. This later contrast parameter computes the Shannon entropy according to the following equation:

$$\text{Shanon} \ \ E \ \ = \sum_{i=1}^{n} \left[x_t^2(i) \log \left(x_t^2(i) \right) \right] \tag{1}$$

When $X_t^2(i) = 0$, let $\log(X_t^2(i)) = 0$. n is the number of samples of the input time series. It allows to compress the data and to underline area presenting contrast. Similarly, we compute also the Energy entropy according to the following equation:

$$E = \sum_{i=1}^{n} \log \left(x_t^2(i) \right) \tag{2}$$

When $X_t^2(i) = 0$, let $\log(X_t^2(i)) = 0$. n is the number of samples of the input time series.

As an example, Fig. 3b shows the best contrasted image, obtained for sample 1 in the THz frequency domain by using energy entropy technique. As a comparison of contrast data, this THz contrast image is compared to the 3D reconstructed X-Ray surface (cf. Fig. 3c).

First, THz contrast image shows the presence of inhomogeneity of recorded intensities in the wax body (white spots). It is a direct consequence of when imaging with terahertz waves in reflection mode, surface morphology, or irregularity are visible. It is not demonstrated yet that it is due to the presence of foreign micro or milli grains in the wax constituents or if these white spots are only induced by refraction effect. However, we also observe the same surface features when imaged with X-Ray. Indeed, on Fig. 3b, c (which is an X-Ray reconstructed surface), we can recognize the central pattern with both techniques. Conversely, we cannot
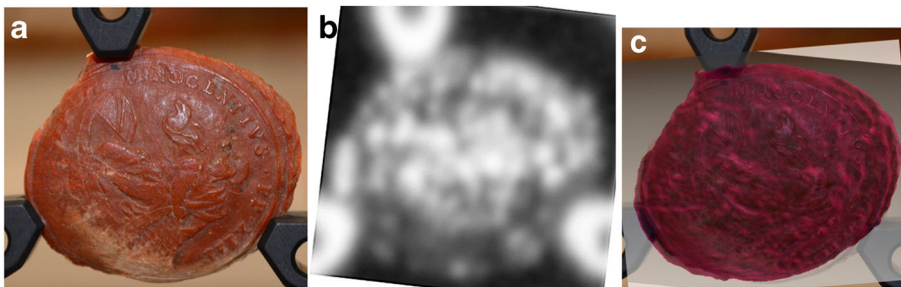
Fig. 3 a Papal seal. b THz energy entropy as a parameter. c X-Ray reconstructed upper surface. AD29, 28 Fi 1. Sample 1

decrypt the letters printed in the wax around the edges or clearly distinguish the different drawings.

3.2 Hamburg Town Seal. (Sample 2)

First, we export, from X-Ray tomography results reported in Fig. 4, some typical pictures of sample 2. We can display an internal slice (XY-plane orthonormal to the Z-axis) of the sample. We note on X-Ray images that several defects are clearly visible as black holes. For example, there is an elongated track which could be a cavity located just below the parchment and a circular mark similar to a cavity (see Fig. 4d). The size of the cavity is estimated about 3 mm in length.

For this sample, terahertz imaging and tomography have been performed in reflection mode, from the both sides. The useful frequency range for this sample is from 0.1 to 2.5 THz. X and Y acquisition steps have been set up to 0.25 mm. This large size sample, relative to the acquisition step, results in the acquisition of several Giga-signals to be analyzed both in time domain and frequency. To be studied efficiently, we implement an ad hoc automated processing sequence composed of i) meta-data determination from both acquired THz data domains and ii) an image-based segmentation extracting the different volumes of interest (VOI) composing the sample. It has been studied in details in [26] for THz continuous wave imaging. It is directly applied to extract TDS-THz meta-data. Meta-data computation, step i), is mainly based on optimized classification methods able to extract relevant series of physical parameters among a large quantify of collected data, thanks to the specific physical THz-beam interactions with matter in diverse regions of the sample.

For example, Fig. 5b represents the high contrasted image by choosing the half width half maximum as parameter. In our case, the "half width" of the "half maximum" is generally used in signal processing to define a frequency bandwidth as "width of frequency range" where less than half the signal power is attenuated.

This image surface reveals quite nice details, such as the three towers, despite the irregularity of the sample. In frequency domain, different data processing is available and reveals different information at different resolutions. For instance, Fig. 5c is the result of the 2 THz FFT amplitude values and Fig. 5d corresponds to the image obtained by Shannon entropy of overall intensities.

Also, some details are visible on the circumference of the seal where the inscription was inserted. No clear defect is revealed in depth since the maximum of contrast is provided by the different thicknesses of the engraved tower patterns. From front side investigation, it is worth mentioning that no defect is certainly detected since the unflatten surface induces too important time domain intensity variations so that no clear correlation is found between signal and defect
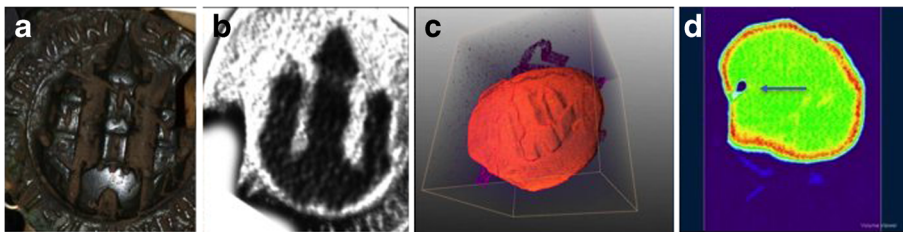
Fig. 4 X-Ray characterization. **a** Picture of the seal. **b** Representation of the reconstructed surface. **c** 3D visualization. **d** An X-Ray slice with a localized defect with an arrow inside the seal
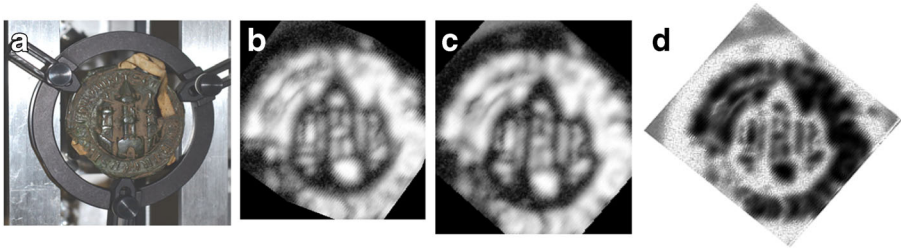
Fig. 5 **a** Picture of sample 2. **b** Half width–half maximum Image. **c** Best frequency (2.1THz). **d** Shannon entropy as contrast parameter

localization. Conversely from the back-side measurements, the large cavity reported in Fig. 4d can unambiguously be detected by THz-TDS. Indeed, Fig. 6a represents the time domain at the precise position of the cavity. The reflected signal is very low since signal losses occur due to geometrical effects. Nevertheless, the two peaks observed several times within different image acquisitions, are the signature of a reflection into the internal cavity. The pair of peaks (highlighted with a red arrow in Fig. 6a) is correlated to the two first interfaces (i.e., air-wax and wax-cavity). Moreover, the time between the two peaks is related to the position of the hole versus the external surface. Then, the position can be estimated between 50 and 100 μm under the surface. The second peak (positioned with the blue arrow) is about 15–20 ps, making the diameter of the cavity in the few millimeter range. These peaks may correspond to internal reflections on multiple interfaces. We also denote a 180° phase shift of a second peak, which is relevant of reflection with a lower index medium.

3.3 Great seal of France (Sample 3)

Great seal of France X-Ray acquisition results is depicted on Fig. 7. Especially, Fig. 7b shows a 3D visualization of the seal with transparency. We can follow inside the seal, the way taken by the strings during the seal elaboration. Particularly interesting, the strings are shared in two different parts and completely crosses through the sample. We can note that the person who made the seal made efforts by combinations of multiple nodes so that the string removal from the seal cannot be done without destroying it. Moreover, we can recognize the character
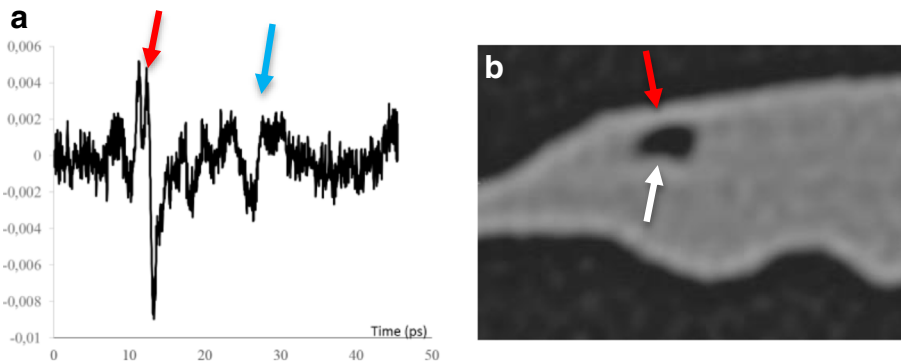
Fig. 6 **a** Time domain recorded close to the defect position. The main peak is split due to multiple reflection inside the cavity. **b** X-Ray image of the defect, the different interfaces are shown with arrows
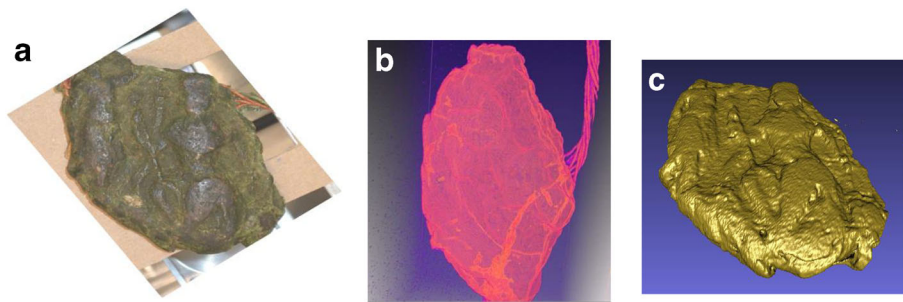
Fig. 7 **a** Picture of the royal seal CT. AD29, 28 Fi 2. **b** X-Ray CT detail of the silken cord inside the seal. **c** Reconstructed surface with X-Ray CT

holding the scepter on the X-Ray surface rendering reported in Fig. 7c. Globally on this sample, X-Ray analysis does not reveal significant fracture or inner cracks.

For that sample, terahertz imaging cannot bring complementary analysis with respect to X-ray analysis. This is due to the high surface irregularities making reflection data impossible to interpret. Indeed, reflected beams are not collected efficiently so that data cannot be referenced correctly for a fair and accurate analysis.

3.4 Personnal Seal, Guyomar de Lesguen (Sample 4)

Another typical feature often found in sigillography, and in particular in the Guyomar de Lesguen seal, is the presence of parchment. Typically, a parchment is an animal skin which underwent a processing without tanning. Sheep or goat is commonly used, whereas the well-known finer quality and more expensive vellum (newborn calf or stillborn), is mainly reserved for princely manuscripts or for the most solemn diplomatic documents. About the pendent seals of the twelfth and early thirteenth centuries, deeds specify sometimes that they are sealed on leather strips of deer.

Inside the seal, the parchment obviously remains hidden to optical inspection but it could appear by terahertz or X-Ray imaging, if the contrast is sufficient to discriminate it with the matrix material. In such a case, the parchment entire path can be followed into the seal. Then, inner inspection may help to determine, particularly, if the parchment is torn and if the tie risks to break. Specially, for this seal, we performed THz-time domain imaging and X-Ray Micro CT to detect the eventual defects around the parchment.

By THz imaging and spectroscopy, we characterized different parchments and we found that the discrimination is difficult because all the different materials have similar dielectric responses [27]. Then, echoes from different interfaces are very low and difficult to extract from noise. So, we do not succeed to visualize the parchment within the sample 4 by THz imaging and even with the basic medical X-Ray scanner we used for the previous experiments.

To complete the study, and particularly, the detection of defects with size lower than 100 μm, a micro-focus X-Ray tomography, was realized. The source illuminates the object, and a flat panel X-Ray detector collects magnified projection images. Based on hundreds of angular views acquired while the object rotates, a computer synthesizes a stack of virtual cross section slices through the object. We obtained 1670 slices, and then we can extract surface orthoslices and volume rendering.

Figure 8 shows different slices putting in evidence the very large numbers of micro fractures inside the seal.

Currently in materials science, crack mechanics is an important tool for understanding and improving the mechanical performance of materials. It may help to discover the causes of failures or to verify theoretical failure predictions with both real life and mechanic elasticity hypotheses [28]. Typically, the analysis of microscopic defects present in materials is often a way to investigate the origin of macroscopic mechanical failure. This kind of material analysis at micro-scale can be processed in order to assess the impact of parchment inclusion in a seal. In the case of the Guyomar de Lesguen seal, we can denote an air gap layer present all around the parchment (cf. Fig. 8). It was probably produced during the wax melting and freezing procedure, and it is certainly due to the inhomogeneity of the foreign objects inserted within the wax. We also observed a lot of fractures, starting from the parchment and going to the external edges of the seal. Finally, we also note some cavities, but contrary to fractures, we cannot assume that they are a consequence of parchment insertion in the seal.

4 Conclusion

In this study, we have shown that both X-Ray and terahertz imaging are useful techniques and provide complementary information. Moreover, they are particularly interesting when working with archeological samples because there is no need to manipulate the object and the measurement is made without any contact.

On the one hand, X-Ray imaging gives a good spatial resolution even in low density materials. The contrast between the various materials (parchment or silken fibers and wax) is sufficient to perform labeling and to evaluate the fragility of the sample around the parchment for instance. In addition, little fractures can be found using X-Ray micro CT, globally assessing the seal conservation state.

On the other hand, we have demonstrated throughout this study that, such as X-Ray imaging, THz can be used for the nondestructive evaluation of original and very fragile seals. Moreover, we
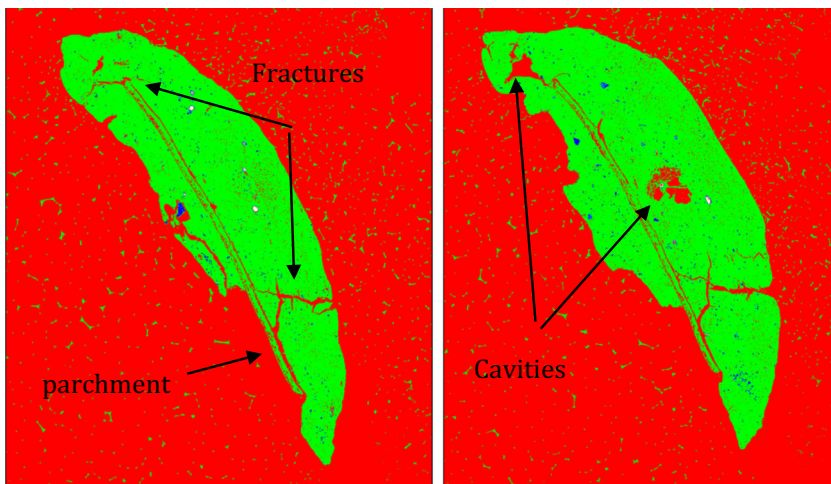
Fig. 8 X-Ray images of the seal: different fractures are clearly distinguished

have shown that THz analysis is a useful complementary technique for the surface investigation of soft material. Indeed, THz imaging and spectroscopy have been used to extract surface or subsurface information. However, the seal thicknesses are usually larger than several millimeters, and the inhomogeneity of the wax material, added to the important surface irregularities, leads to an elusive challenge for THz analysis in depth. Nevertheless, THz absorbance is low enough to analyze spectral properties of foreign inclusion. Moreover, since THz-pulse imaging measures the time of flight when traveling through the sample, it becomes feasible to detect cavities under a few millimeter layer of old wax materials, without adopting a tomography approach. Finally, THz spectroscopy could even give information on dielectric response of different waxes and their similarities between different samples seals impressions in a study concerning the wax supplies within a chancery. Thus, Terahertz radiation offers a totally noninvasive diagnostic imaging for historic testimonies.

To conclude, THz and X-Ray should be commonly used together in order to obtain the more complete results when imaging objects. However, in the case of historical and archeological samples, THz is preferred for its status as a nonionizing technique, which does not destroy biochemical fingerprints of biological materials for eventual upcoming analysis. Thus, the study, the appreciation, and, in particular, the conservation of the sealed records will find a tool in THz to take part in the sustainability and better knowledge of this historical patrimony.

Reference

1. K. Fukunaga, Y. Ogawa, S. i. Hayashi, and I. Hosako, Application of terahertz spectroscopy for character recognition in a medieval manuscript, IEICE Electronics Express **5**, 223–228 (2008).
2. J. B. Jackson, M. Mourou, J. F. Whitaker, I. N. Duling, III, S. L. Williamson, M. Menu, and G. A. Mourou, "Terahertz imaging for non-destructive evaluation of mural paintings," Opt. Commun. **281**, 527–532 (2008).
3. E. Abraham, A. Younus, A. El Fatimy, J.-C. Delagnes, E. Nguéma, and P. Mounaix, "Broadband terahertz imaging of documents written with lead pencils," Opt. Commun. **282**, 3104–3107 (2009).
4. A. J. Adam, P. Planken, S. Meloni, and J. Dik, "TeraHertz imaging of hidden paint layers on canvas," Optics Express **17**, 3407–3416 (2009).
5. K. Fukunaga, and M. Picollo, "Terahertz spectroscopy applied to the analysis of artists' materials," Applied Physics A **100**, 591–597 (2010).
6. L. Öhrström, A. Bitzer, M. Walther, and F. J. Rühli, "Technical note: Terahertz imaging of ancient mummies and bone," American Journal of Physical Anthropology **142**, 497–500 (2010).
7. K. Fukunaga, and I. Hosako, "Innovative non-invasive analysis techniques for cultural heritage using terahertz technology," Comptes Rendus Physique **11**, 519–526 (2010).
8. J. B. Jackson, J. Bowen, G. Walker, J. Labaune, G. Mourou, M. Menu, and K. Fukunaga, "A survey of terahertz applications in cultural heritage conservation science," IEEE Transactions on Terahertz Science and Technology **1**, 220–231 (2011).
9. K. Krügener, M. Schwerdtfeger, S. F. Busch, A. Soltani, E. Castro-Camus, M. Koch, and W. Viöl, "Terahertz meets sculptural and architectural art: Evaluation and conservation of stone objects with T-ray technology," Scientific reports **5**, 14842 (2015).
10. J. P. Guillet, B. Recur, L. Frederique, B. Bousquet, L. Canioni, I. Manek-Hönninger, P. Desbarats, and P. Mounaix, "Review of Terahertz tomography techniques," J Infrared Milli Terahz Waves **35**, 382–411 (2014).
11. X. C. Zhang, "Three-dimensional terahertz wave imaging," Philosophical Transactions of the Royal Society of London Series a-Mathematical Physical and Engineering Sciences **362**, 283–298 (2004).

12. S. Wang, and X. Zhang, "Pulsed terahertz tomography," Journal of Physics D: Applied Physics **37**, R1 (2004).

13. K. L. Nguyen, M. L. Johns, L. F. Gladden, C. H. Worrall, P. Alexander, H. E. Beere, M. Pepper, D. A. Ritchie, J. Alton, S. Barbieri, and E. H. Linfield, "Three-dimensional imaging with a terahertz quantum cascade laser," Optics Express **14**, 2123–2129 (2006).

14. M. Herrmann, F. Platte, K. Nalpantidis, R. Beigang, and H. M. Heise, "Combination of Kramers–Kronig transform and time-domain methods for the determination of optical constants in THz spectroscopy," Vibrational Spectroscopy **60**, 107–112 (2012).

15. M. Fabre, *Sceau médiéval: analyse d'une pratique culturelle* (Editions L'Harmattan, 2001).

16. J. El Haddad, B. Bousquet, L. Canioni, and P. Mounaix, "Review in terahertz spectral analysis," TrAC Trends in Analytical Chemistry **44**, 98–105 (2013).

17. P. Mounaix, A. Younus, J.-C. Delagnes, E. Abraham, L. Canioni, and M. Fabre, "Spectroscopy and terahertz imaging for sigillography applications," Journal of the European Optical Society-Rapid publications **6** (2011).

18. A. Brahm, M. Kunz, S. Riehemann, G. Notni, and A. Tuennermann, "Volumetric spectral analysis of materials using terahertz-tomography techniques," Applied Physics B-Lasers and Optics **100**, 151–158 (2010).

19. B. Recur, J.-P. Guillet, I. Manek-Hönninger, J.-C. Delagnes, W. Benharbone, P. Desbarats, J.-P. Domenger, L. Canioni, and P. Mounaix, "Propagation beam consideration for 3d thz computed tomography," Optics express **20**, 5817–5829 (2012).

20. J. Perraud, A. Obaton, J. Bou-Sleiman, B. Recur, H. Balacey, F. Darracq, J. Guillet, and P. Mounaix, "Terahertz imaging and tomography as efficient instruments for testing polymer additive manufacturing objects," Appl. Optics **55**, 3462–3467 (2016).

21. F. Ospald, W. Zouaghi, R. Beigang, C. Matheis, J. Jonuscheit, B. Recur, J.-P. Guillet, P. Mounaix, W. Vleugels, and P. V. Bosom, "Aeronautics composite material inspection with a terahertz time-domain spectroscopy system," Optical Engineering **53**, 031208–031208 (2014).

22. S. Fan, E. P. J. Parrott, B. S. Y. Ung, and E. Pickwell-MacPherson, "Calibration method to improve the accuracy of THz imaging and spectroscopy in reflection geometry," Photon. Res. **4**, A29-A35 (2016).

23. M.Fabre, Collection d'empreintes de sceaux détachés et de moulages, Quimper, Archives départementales du Finistère, 2011.

24. I. Takeuchi, K. Shimakura, H. Ohtake, J. Takayanagi, K. Tomoda, T. Nakajima, H. Terada, and K. Makino, "Nondestructive analysis of structure and components of tablet coated with film by the usage of terahertz time-domain reflection spectroscopy," J Pharm Sci **103**, 256–261 (2014).

25. T. Löffler, K. Siebert, S. Czasch, T. Bauer, and H. G. Roskos, "Visualization and classification in biomedical terahertz pulsed imaging," Physics in Medicine and Biology **47**, 3847 (2002).

26. H. Balacey, B. Recur, J.-B. Perraud, J. B. Sleiman, J.-P. Guillet, and P. Mounaix, "Advanced Processing Sequence for 3-D THz Imaging," IEEE Transactions on Terahertz Science and Technology **6**, 191–198 (2016).

27. R. Durand, J. Guillet, B. Recur, P. Mounaix, M. Fabre, and S. Genot, "X-ray versus 3D terahertz imaging for sigillography science," in *Infrared, Millimeter, and Terahertz Waves (IRMMW-THz), 2013 38th International Conference on* (IEEE2013), pp. 1–1.

28. H. L. Ramandi, P. Mostaghimi, R. T. Armstrong, M. Saadatfar, and W. V. Pinczewski, "Porosity and permeability characterization of coal: a micro-computed tomography study," International Journal of Coal Geology **154**, 57–68 (2016).